

## Towards a Global QCD Analysis of Fragmentation Functions at Next-to-Next-to-Leading Order Accuracy

Ignacio Borsa<sup>✉\*</sup> and Rodolfo Sassot<sup>✉†</sup>

*Departamento de Física and IFIBA, Facultad de Ciencias Exactas y Naturales, Universidad de Buenos Aires, Ciudad Universitaria, Pabellón 1, 1428 Buenos Aires, Argentina*

Daniel de Florian<sup>‡</sup>

*International Center for Advanced Studies (ICAS) and IFICI, UNSAM, Campus Miguelete, 25 de Mayo y Francia, 1650 Buenos Aires, Argentina*

Marco Stratmann<sup>§</sup> and Werner Vogelsang<sup>||</sup>

*Institute for Theoretical Physics, University of Tübingen, Auf der Morgenstelle 14, 72076 Tübingen, Germany*

 (Received 12 February 2022; revised 29 April 2022; accepted 9 June 2022; published 1 July 2022)

We carry out a global QCD analysis of parton-to-pion fragmentation functions at next-to-next-to-leading order (NNLO) accuracy by performing a fit to the combined set of single-inclusive electron-positron annihilation and, for the first time, semi-inclusive deep-inelastic scattering multiplicity data. For the latter, we utilize the approximate NNLO QCD corrections that were derived recently within the threshold resummation formalism. We explore the impact of the NNLO corrections on the description of the semi-inclusive deep-inelastic scattering datasets in various kinematic regimes and on the resulting pion fragmentation functions.

DOI: [10.1103/PhysRevLett.129.012002](https://doi.org/10.1103/PhysRevLett.129.012002)

*Introduction.*—Fragmentation functions (FFs) constitute a crucial building block in perturbative calculations of scattering cross sections with detected final-state hadrons [1]. In the presence of a sufficiently large energy scale, QCD factorization allows one to isolate the physics describing the transition of an outgoing parton to an observed, colorless hadron from the hard scattering process that produced the parton [2]. The parton-to-hadron FFs, which precisely describe this transition are a unique manifestation of the nonperturbative formation of QCD final states via “hadronization,” and hence offer insights central to our understanding of the strong interactions. The wide range of applications of FFs includes modern studies of the nucleon’s spin structure [3], as well as investigations of modifications of hadron production rates in scattering processes involving heavy nuclei [4].

FFs are process-independent quantities and thus can be determined from data by means of a global QCD analysis [5]. The energy scale dependence of FFs can be computed perturbatively as an expansion in the strong coupling and is currently known up to next-to-next-to-leading order (NNLO) accuracy [6,7]. Given the importance of FFs,

their global analysis has enjoyed considerable theoretical interest recently, resulting in various new sets for different kinds of identified hadrons [8–18]. But, unlike the case of parton distribution functions (PDFs), global analyses of FFs have been essentially limited to the next-to-leading order (NLO) accuracy of QCD perturbation theory. This is due to the lack of NNLO computations for the cross sections for some of the most relevant processes sensitive to FFs, i.e., semi-inclusive deep-inelastic scattering (SIDIS) and single-inclusive hadron production in proton-proton ( $pp$ ) collisions. As a result, except for heavy-flavor [19] and transverse-momentum dependent [20] fragmentation functions, the few NNLO extractions of FFs [13,16,17,21] are currently based solely on single-inclusive electron-positron annihilation (SIA) data. These studies found the NNLO corrections to be small in the kinematic regime where SIA data exist. Reference [22] extended the analysis of SIA data by including all-order resummation effects at small hadron momentum fractions, again observing very modest effects.

The purpose of our Letter is to perform a first “proof-of-principle” *global* analysis of FFs at NNLO accuracy, based on the available SIA [23] and—for the first time in a NNLO framework—the SIDIS data for identified charged pions of [24,25]. Such an analysis is now possible, thanks to the recent derivation of approximate NNLO corrections for SIDIS in [26]. These corrections were obtained within the threshold resummation formalism, expanding the all-order

---

*Published by the American Physical Society under the terms of the Creative Commons Attribution 4.0 International license. Further distribution of this work must maintain attribution to the author(s) and the published article’s title, journal citation, and DOI. Funded by SCOAP<sup>3</sup>.*

resummed results to NNLO accuracy in the strong coupling. They are approximate in the sense that they contain all the dominant contributions associated with the emission of soft gluons near threshold (and even some subdominant contributions), but do not yet constitute the full NNLO results. Nevertheless, they should be readily suited for an initial phenomenological NNLO analysis of SIDIS data in terms of FFs.

Several factors motivate us to perform this study. First, the precision of current LHC experiments and much anticipated measurements with identified hadrons at the future Electron-Ion Collider (EIC) [27] will make the development of a framework for a full global analysis of FFs at NNLO accuracy, and encompassing all available probes, mandatory. Although this goal is still rather far off (for example, NNLO corrections to hadron production in  $pp$  scattering are not yet available; see, however, [28,29] for recent progress), we believe that adding SIDIS to the NNLO framework marks an important step in this direction, demonstrating that global NNLO analyses of FFs are possible in principle. Second, already at this stage one can examine the question whether the very modest NNLO effects seen in the SIA-only analysis also recur when adding SIDIS data to the analysis. This addresses the rather important question of perturbative stability of the global extraction of FFs. Finally, based on our first exploratory analysis we will also be able to delineate the kinematic regions where the NNLO corrections to SIDIS matter most. This may also shed light on the question in what regions the approximate NNLO terms derived in [26] are sufficiently accurate, or where a full NNLO calculation for SIDIS may be required.

*Scope and setup of the analysis.*—Pions are the most copiously produced hadrons and, hence, the corresponding datasets are the most precise ones at hand. The COMPASS [25] and HERMES [24] SIDIS results are presented in terms of multiplicities, i.e., normalized to the fully inclusive deep-inelastic cross section. While all COMPASS data were taken in scattering off deuterium, HERMES has presented results both for proton and deuterium targets. The two fixed-target experiments have been performed at rather moderate center-of-mass (c.m.) system energies  $\sqrt{s}$ . As a consequence, they cover only limited ranges in the photon's virtuality  $Q^2$  and the Bjorken variable  $x$ . SIDIS is characterized by an additional variable  $z$ , defined as the fraction of the virtual photon's energy carried by the observed hadron in the target rest frame. Since the bulk of the available SIDIS data sits at moderate  $Q^2$ , we might expect NNLO corrections to be more pronounced than for SIA where most data were taken on the  $Z$ -boson resonance. There are also plenty of SIDIS data at moderate-to-large values of  $x$  and/or  $z$  where the threshold approximation for the NNLO cross sections should work very well.

For consistency, we disregard the wealth of  $pp$  data with identified pions [30] since the relevant NNLO corrections

are not yet known. In existing NLO fits, these data serve as the main constraint for the gluon-to-pion FF which is otherwise largely unconstrained. This implies that our obtained set of NNLO pion FFs solely from SIA and SIDIS probes is not meant to replace the results of existing NLO global analyses, although it may still be useful for calculations requiring FFs at NNLO.

In the technical analysis, we closely follow the general framework outlined and used in previous global analyses of FFs by the DSS group [5,10,18]. Specifically, the fragmentation of a parton of flavor  $i$  into a positively charged pion is parametrized at an initial scale of  $Q_0 = 1$  GeV as

$$D_i^{\pi^+}(z, Q_0) = N_i \frac{\sum_{j=1}^3 \gamma_{ij} z^{\alpha_{ij}} (1-z)^{\beta_{ij}}}{\sum_{j=1}^3 \gamma_{ij} B(2 + \alpha_{ij}, 1 + \beta_{ij})}, \quad (1)$$

where  $B(a, b)$  is the Euler beta function and we assume as usual  $D_q^{\pi^-} = D_q^{\pi^+}$ . Since the data cannot constrain all the free parameters in Eq. (1), we adopt the same assumptions as in [8,18]. Additionally, as the gluon FF  $D_g^{\pi^+}$  is only weakly constrained, we stick to a simple functional form with  $\gamma_{g2} = \gamma_{g3} = 0$ .

As in [18], our analysis implements a Monte Carlo sampling strategy to obtain an ensemble of replicas of the FFs which provides a faithful representation of their underlying probability distributions and simplifies the estimation of errors. We do not investigate the reduction of the factorization and renormalization scale uncertainties at NNLO accuracy and set all scales equal to the relevant experimental value of  $Q$  throughout. The scale dependence was studied in Ref. [26] and found to be noticeably smaller at NNLO than at NLO for typical COMPASS kinematics and  $z \gtrsim 0.3$ .

The optimum values for the free parameters in Eq. (1) are determined using a standard  $\chi^2$  minimization procedure. The scale evolution of the FFs up to NNLO and the computation of the SIA cross sections utilizes the codes developed in Refs. [21,31]. We note that for the NNLO fit we also compute the inclusive DIS cross section in the denominator of the SIDIS multiplicity at NNLO, using the numerical implementation in [32]. We adopt the NNPDF4.0 [33] set of PDFs along with its strong coupling  $\alpha_s$ , and consider the quoted uncertainties in quadrature in the value for  $\chi^2$ .

All numerical calculations are efficiently performed in Mellin moment space, where also the approximate NNLO corrections of [26] were derived. For the SIDIS cross section this amounts to performing a double Mellin inverse transform. To facilitate the computational burden, the integration related to the PDF dependence of the SIDIS cross section can be carried out once prior to the actual fit and stored in grids [34]. A typical  $\chi^2$  minimization at NNLO accuracy is then performed in about 20 min on a single CPU core. Clearly, our efficient Mellin technique

TABLE I. Partial and total  $\chi^2$  values per data point for the sets included in our NLO and NNLO global fits for different lower cuts on  $Q^2$ .

Experiment	$Q^2 \geq 1.5 \text{ GeV}^2$			$Q^2 \geq 2.0 \text{ GeV}^2$			$Q^2 \geq 2.3 \text{ GeV}^2$			$Q^2 \geq 3.0 \text{ GeV}^2$		
	Data points	NLO	NNLO	Data points	NLO	NNLO	Data points	NLO	NNLO	Data points	NLO	NNLO
SIA	288	1.05	0.96	288	0.91	0.87	288	0.90	0.91	288	0.93	0.86
COMPASS	510	0.98	1.14	456	0.91	1.04	446	0.91	0.92	376	0.94	0.93
HERMES	224	2.24	2.27	160	2.40	2.08	128	2.71	2.35	96	2.75	2.26
Total	1022	1.27	1.33	904	1.17	1.17	862	1.17	1.13	760	1.16	1.07

will allow for a full-fledged NNLO global analysis of FFs in the future including also  $pp$  scattering at NNLO accuracy.

*Results and discussion.*—In Table I we present the results of a series of global fits at NLO and NNLO accuracy to the combined set of SIA and SIDIS data with gradually increasing cuts on  $Q^2$  from its minimum value of  $1.5 \text{ GeV}^2$ . We observe that for  $Q^2 \geq 1.5 \text{ GeV}^2$  the description of the SIDIS data deteriorates by including the approximate NNLO corrections, particularly in the case of COMPASS. However, discarding bins with low values of  $Q^2$  systematically leads to a better global fit at NNLO, surpassing the quality of the NLO result in terms of the overall  $\chi^2$  already for  $Q^2 \geq 2 \text{ GeV}^2$ . Once we demand  $Q^2 \geq 3 \text{ GeV}^2$ , the NNLO fit shows not only a much improved total  $\chi^2$  value, but also a better quality of the description of both SIDIS datasets. Interestingly, the NNLO fit shows significant improvements also in case of the SIA data which all sit above the  $Q^2$  cuts we have implemented, in contrast to what was found previously in fits based solely on SIA data [21]. This is to be attributed to the additional “pull” by the SIDIS data.

Any lower cut in  $Q^2$  is kinematically correlated with the lowest value of  $x$  accessible in the two SIDIS experiments. For instance, demanding  $Q^2 \geq 3 \text{ GeV}^2$  removes all COMPASS data in the range  $0.004 \leq x \leq 0.02$ , and about half of the data with  $0.02 \leq x \leq 0.06$ . Because of the lower c.m. system energy of HERMES, its number of data points is reduced even more strongly when increasing the lower  $Q^2$  cut. Previous global analyses [5,10,18] suggest that there are tensions between the HERMES and COMPASS SIDIS datasets. It appears that this tension is somewhat mitigated by inclusion of the NNLO terms and also by increasing the lower cut on  $Q^2$ , although it still persists at some level, as seen from the relatively large values of  $\chi^2$  relative to the number of data points for HERMES.

Figures 1 and 2 compare our NLO and NNLO results to the COMPASS and HERMES SIDIS multiplicities in a few representative bins in  $x$ . We normalize all results to the baseline NLO fit with  $Q^2 \geq 1.5 \text{ GeV}^2$ . Using this cut also at NNLO tends to give a result that slightly overestimates the SIDIS multiplicities, especially at lower values of  $x$  or  $Q^2$ , which is the reason for the larger  $\chi^2$  value seen for this

cut in Table I. This changes once we increase the cut to  $Q^2 \geq 3.0 \text{ GeV}^2$ , also shown for NNLO in Figs. 1 and 2, where a clearly improved description of the multiplicities is observed. Note that we show the NNLO results for this cut even for the  $Q^2$  values below  $3.0 \text{ GeV}^2$ , so that the deterioration in the region not included in that fit can be seen.

It is very encouraging that our NNLO analysis based on the approximate NNLO corrections for SIDIS shows an overall improvement in  $\chi^2$  relative to NLO once we go beyond  $Q^2 = 2 \text{ GeV}^2$ . It is an interesting question, however, why the situation is opposite when the lower cut  $Q^2 \geq 1.5 \text{ GeV}^2$  is used. We first note that the lack of improvement at NNLO when low  $Q^2$  are admitted, as well as the progressive improvements with stricter cuts on  $Q^2$ , are not due to the tensions between the different sets of SIDIS data mentioned above. In fact, similar results as in Table I are also obtained in fits using exclusively SIA and COMPASS data.

Two other possible explanations come to mind. Clearly, values of  $Q^2$  below  $3 \text{ GeV}^2$  or even  $2 \text{ GeV}^2$  raise concerns about the applicability of a leading-power factorized framework that describes the cross section in terms of just PDFs, FFs, and perturbative hard-scattering cross sections. It is quite possible that the trends seen at the lowest  $Q^2$  values indicate the onset and perhaps even dominance of power corrections, very little about which is known theoretically for SIDIS. In a similar vein, at low  $Q^2$  one may question the dominance of the current fragmentation regime [35]. Even at a practical level the region  $Q^2 < 2 \text{ GeV}^2$  is tedious in our analysis: All modern sets of PDFs incorporate a fairly large  $Q^2$  cut on the fixed-target DIS data entering their global analysis. When computing the SIDIS multiplicities we therefore need to resort to extrapolations of the PDF sets outside the region of their applicability for a considerable amount of the available data, in particular, for HERMES kinematics [36]. The cut  $Q^2 \geq 3.0 \text{ GeV}^2$  helps to mitigate this otherwise unavoidable—and hard to quantify—ambiguity stemming from the choice of PDFs. We have verified, however, that replacing the NNPDF4.0 set [33], adopted throughout our Letter, by the latest MSHT set of PDFs [37] does not significantly change our results and conclusions.



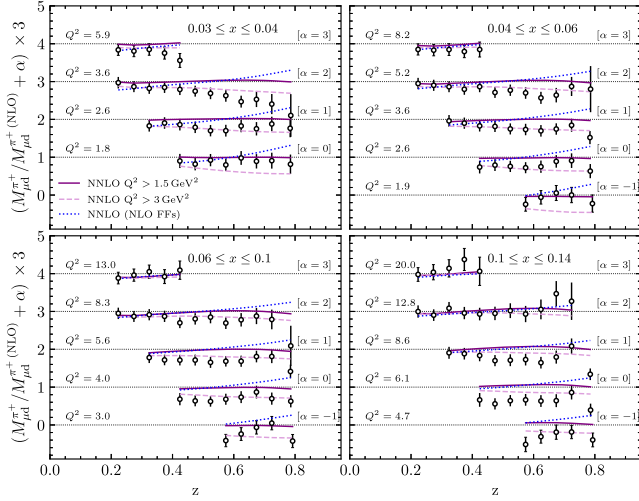


FIG. 1. Comparison of our NLO and NNLO fits with  $Q^2 \geq 1.5 \text{ GeV}^2$  to the COMPASS  $\pi^+$  multiplicities for some representative bins of  $x$ , normalized to the NLO results. The dashed lines show the change of the NNLO fit when the  $Q^2 \geq 3 \text{ GeV}^2$  cut is implemented. For a “test calculation” represented by the dotted lines we have used the FFs from the NLO fit in the NNLO calculation (see text). For better clarity, all results are scaled and shifted by constant factors.

The other possibility is that the approximate NNLO corrections for SIDIS might miss some significant contributions not associated with the threshold regime. Since threshold resummation only addresses the region of large  $x$  and  $z$  such nonthreshold contributions, if sizable, could indeed make the approximate NNLO description unreliable for low values of  $x$  and hence  $Q^2$ . To see whether there are indications of such a behavior, we have redone the NNLO calculation with  $Q^2 \geq 1.5 \text{ GeV}^2$ , but using the FFs obtained in the NLO fit. The corresponding results are also shown in Figs. 1 and 2. Here the idea is that the ratio to the NLO multiplicity will help identify any regions where sizable NNLO corrections arise just from the partonic hard-scattering cross sections. As one can see, for large values of  $z$  there are significant enhancements at NNLO. The threshold logarithms are precisely expected to generate such enhancements. However, we also observe downward NNLO corrections at lower values of  $z$ , and here especially at lower  $Q^2$  and hence  $x$ . Clearly, based on this feature alone we cannot judge whether this reduction of the cross section at NNLO is an artifact of the near-threshold approximation. This would only become possible with a future full NNLO calculation for SIDIS. For now we just issue a word of caution concerning this point.

We finally consider the FFs that our fits produce. Figure 3 shows the functions for  $\pi^+$  production, evolved to  $Q^2 = 100 \text{ GeV}^2$ , for  $u_{\text{tot}} \equiv u + \bar{u}$ ,  $d_{\text{tot}} \equiv d + \bar{d}$ ,  $d = \bar{u}$ , and the flavor singlet combination  $\Sigma$ , along with uncertainty estimates at 68% C.L. (confidence level). We show the resulting NLO and NNLO distributions both for

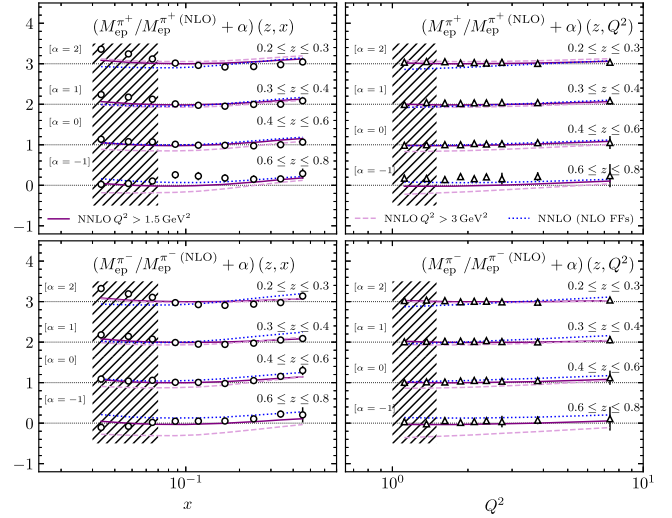


FIG. 2. Same as in Fig. 1 but for the HERMES  $\pi^\pm$  SIDIS data on a proton target, for two different projections of the data. The shaded areas indicate the regions excluded from the fit by the  $Q^2 \geq 1.5 \text{ GeV}^2$  cut.

$Q^2 \geq 1.5 \text{ GeV}^2$  and  $Q^2 \geq 3 \text{ GeV}^2$  in the fit. All distributions shown are well constrained by our new global fit to SIA and SIDIS data at NNLO accuracy, while the gluon and strange quark FFs remain largely undetermined. The rightmost panels of Fig. 3, which present the ratios of the NNLO quark FFs over the NLO ones, best illustrate the distinct,  $z$ -dependent pattern of modifications needed when switching from NLO to NNLO accuracy. The most significant feature at NNLO is the suppression of the FFs for  $z \gtrsim 0.6$ , needed to counteract the enhancements in the partonic cross sections at large  $z$  due to the threshold logarithms. We note that the cut  $Q^2 \geq 3.0 \text{ GeV}^2$  mainly

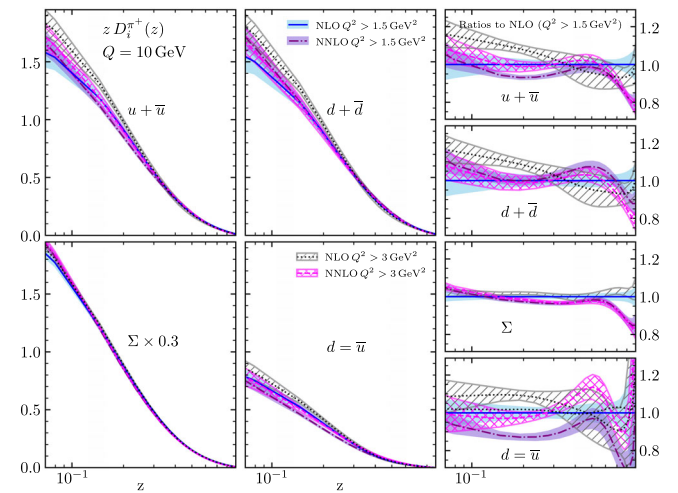


FIG. 3. Our NLO and NNLO  $\pi^+$  FFs for  $u_{\text{tot}}$ ,  $d_{\text{tot}}$ ,  $\bar{u}$ , and the flavor singlet combination  $\Sigma$  at  $Q^2 = 100 \text{ GeV}^2$ , with 68% C.L. uncertainty estimates. The rightmost panels give the ratios to our NLO result.

leads to an enhancement of  $u_{\text{tot}}$  below  $z \sim 0.6$  and a largely  $z$  independent increase of the unfavored sea quark FFs. Additionally, while the NLO and NNLO uncertainties are comparable for a  $Q^2$  cut of  $1.5 \text{ GeV}^2$ , imposing the more stringent  $Q^2$  cut leads to a sizable reduction in the NNLO error for  $z \gtrsim 0.2$ .

*Conclusions.*—We have presented the first next-to-next-to-leading order global analysis of parton-to-pion fragmentation functions, based on the existing data on single-inclusive electron-positron annihilation and semi-inclusive deep-inelastic scattering. The cross sections for the latter were obtained using approximate NNLO corrections previously derived within the threshold resummation formalism. Our Letter is motivated by the desire to improve the theoretical framework for the precision analysis of hadron production data. This task appears particularly important in view of the future EIC.

The FFs we find at NNLO are overall close to the NLO ones, indicating good perturbative stability of the processes used for the extraction of PDFs. This is especially true for the flavor singlet and the total up and down quark FFs. As expected, the most noticeable difference at NNLO is the depletion of the FFs in the high- $z$  region.

We have found that the NNLO corrections improve the overall quality of the fit to the data, but do so only when a lower cut of at least  $Q^2 \geq 2 \text{ GeV}^2$  is implemented. With a yet more stringent cut  $Q^2 \geq 3 \text{ GeV}^2$  the NNLO fit becomes markedly better than the NLO one. This may indicate that the low- $Q^2$  regime in SIDIS is not well suited for an analysis in terms of factorized cross sections. The extrapolation of the PDFs beyond the region where they are constrained by data might be an additional source of inconsistencies. That said, also the study of NNLO corrections not directly associated with the threshold regime will deserve further attention in the future. Ultimately a full NNLO calculation for SIDIS will be required to describe future EIC data which will likely be taken in kinematic regions quite far away from the threshold regime. In any case, we believe that our study is an important step on the way to future fully global NNLO analyses of FFs that include also data from hadron production in  $pp$  collisions.

I. B. wishes to thank the University of Tübingen for hospitality during the completion of the work. This work was supported in part by CONICET, ANPCyT, UBACyT, and by Deutsche Forschungsgemeinschaft (DFG) through the Research Unit FOR 2926 (Project No. 40824754).

\*iborsa@df.uba.ar

†sassot@df.uba.ar

‡deflo@unsam.edu.ar

§marco.stratmann@uni-tuebingen.de

||werner.vogelsang@uni-tuebingen.de

[1] J. C. Collins and D. E. Soper, *Nucl. Phys.* **B194**, 445 (1982).

- [2] J. C. Collins, D. E. Soper, and G. F. Sterman, *Adv. Ser. Dir. High Energy Phys.* **5**, 1 (1989).
- [3] See, for instance, D. De Florian, G. A. Lucero, R. Sassot, M. Stratmann, and W. Vogelsang, *Phys. Rev. D* **100**, 114027 (2019).
- [4] See, for instance, R. Sassot, M. Stratmann, and P. Zurita, *Phys. Rev. D* **81**, 054001 (2010).
- [5] D. de Florian, R. Sassot, and M. Stratmann, *Phys. Rev. D* **75**, 114010 (2007).
- [6] A. Mitov, S. Moch, and A. Vogt, *Phys. Lett. B* **638**, 61 (2006).
- [7] A. A. Almasy, S. Moch, and A. Vogt, *Nucl. Phys.* **B854**, 133 (2012).
- [8] D. de Florian, R. Sassot, M. Epele, R. J. Hernández-Pinto, and M. Stratmann, *Phys. Rev. D* **91**, 014035 (2015).
- [9] N. Sato, J. J. Ethier, W. Melnitchouk, M. Hirai, S. Kumano, and A. Accardi, *Phys. Rev. D* **94**, 114004 (2016).
- [10] D. de Florian, M. Epele, R. J. Hernandez-Pinto, R. Sassot, and M. Stratmann, *Phys. Rev. D* **95**, 094019 (2017).
- [11] V. Bertone, S. Carrazza, N. P. Hartland, E. R. Nocera, and J. Rojo (NNPDF Collaboration), *Eur. Phys. J. C* **77**, 516 (2017).
- [12] D. P. Anderle, T. Kaufmann, M. Stratmann, F. Ringer, and I. Vitev, *Phys. Rev. D* **96**, 034028 (2017).
- [13] M. Salajegheh, S. M. Nejad, H. Khanpour, B. A. Kniehl, and M. Soleymaninia, *Phys. Rev. D* **99**, 114001 (2019).
- [14] E. Moffat, W. Melnitchouk, T. C. Rogers, and N. Sato (JAM Collaboration), *Phys. Rev. D* **104**, 016015 (2021).
- [15] R. Abdul Khalek, V. Bertone, and E. R. Nocera, *Phys. Rev. D* **104**, 034007 (2021).
- [16] M. Soleymaninia, H. Abdolmaleki, and H. Khanpour, *Phys. Rev. D* **102**, 114029 (2020).
- [17] H. Abdolmaleki, M. Soleymaninia, H. Khanpour, S. Amoroso, F. Giuli, A. Glazov, A. Luszczak, F. Olness, and O. Zenaiev, *Phys. Rev. D* **104**, 056019 (2021).
- [18] I. Borsa, D. de Florian, R. Sassot, and M. Stratmann, *Phys. Rev. D* **105**, L031502 (2022).
- [19] M. L. Czakon, T. Generet, A. Mitov, and R. Poncelet, *J. High Energy Phys.* **10** (2021) 216.
- [20] M. G. Echevarria, I. Scimemi, and A. Vladimirov, *J. High Energy Phys.* **09** (2016) 004.
- [21] D. P. Anderle, M. Stratmann, and F. Ringer, *Phys. Rev. D* **92**, 114017 (2015).
- [22] D. P. Anderle, T. Kaufmann, M. Stratmann, and F. Ringer, *Phys. Rev. D* **95**, 054003 (2017).
- [23] For a current list of SIA datasets, see, e.g., Ref. [18].
- [24] A. Airapetian *et al.* (HERMES Collaboration), *Phys. Rev. D* **87**, 074029 (2013).
- [25] C. Adolph *et al.* (COMPASS Collaboration), *Phys. Lett. B* **764**, 1 (2017).
- [26] M. Abele, D. de Florian, and W. Vogelsang, *Phys. Rev. D* **104**, 094046 (2021).
- [27] R. Abdul Khalek *et al.*, *arXiv:2103.05419*.
- [28] P. Hinderer, F. Ringer, G. Sterman, and W. Vogelsang, *Phys. Rev. D* **99**, 054019 (2019).
- [29] T. Gehrmann and R. Schürmann, *J. High Energy Phys.* **04** (2022) 031.
- [30] For a current list of  $pp$  datasets, see, e.g., Ref. [18].
- [31] A. Vogt, *Comput. Phys. Commun.* **170**, 65 (2005).

- [32] V. Bertone, S. Carrazza, and J. Rojo, *Comput. Phys. Commun.* **185**, 1647 (2014).
- [33] R. D. Ball, S. Carrazza, J. Cruz-Martinez, L. Del Debbio, S. Forte, T. Giani, S. Iranipour, Z. Kassabov, J. I. Latorre, and E. R. Nocera *et al.*, *Eur. Phys. J. C* **82**, 428 (2022).
- [34] M. Stratmann and W. Vogelsang, *Phys. Rev. D* **64**, 114007 (2001).
- [35] M. Boggione, M. Diefenthaler, S. Dolan, L. Gamberg, W. Melnitchouk, D. Pitonyak, A. Prokudin, N. Sato, and Z. Scalyer, *J. High Energy Phys.* **04** (2022) 084.
- [36] I. Borsa, R. Sassot, and M. Stratmann, *Phys. Rev. D* **96**, 094020 (2017).
- [37] S. Bailey, T. Cridge, L. A. Harland-Lang, A. D. Martin, and R. S. Thorne, *Eur. Phys. J. C* **81**, 341 (2021).